

## Physics and astrophysics with high energy $\nu$ in MACRO<sup>(\*)</sup>

M. SPURIO

for the MACRO Collaboration

*Dipartimento di Fisica dell'Università and INFN - Bologna, Italy*

(ricevuto il 5 Dicembre 1996; approvato il 18 Marzo 1997)

**Summary.** — The events collected with the lower part of the MACRO detector at the Gran Sasso Laboratory have been analyzed looking for neutrino-induced muons. Upward throughgoing events have been measured and the result is compared with Monte Carlo prediction. The first results concerning upward stopping muons and partially contained events are also reported. A search has been made for astrophysical point sources of neutrinos. No point sources have been observed.

PACS 96.40 – Cosmic rays.

PACS 01.30.Cc – Conference proceedings.

### 1. – Introduction

Large underground experiments can detect neutrinos produced by various sources with different energy spectra. For energies up to about 15 MeV, the majority comes from nuclear fusion processes in the Sun. Very rarely, slightly higher-energy neutrinos and antineutrinos of all flavors come in a burst of about 10 s duration from a nearby supernova explosion. For these *low energy* neutrinos, positive results exist: the detection of solar  $\nu_e$  and the detection of the SN1987A  $\bar{\nu}_e$  burst. At higher energy, atmospheric neutrinos dominate. These  $\nu$ 's are the results of the decays of  $\pi^\pm$  and  $k^\pm$  produced by the interactions of cosmic rays in the upper atmosphere. From these processes, we expect that:  $\nu_\mu \sim \bar{\nu}_\mu \sim 2\nu_e$  and  $\nu_e/\bar{\nu}_e \sim \mu^+/\mu^-$ .

Recently, considerable interest has been generated in precise measurements of the flux of atmospheric neutrinos due to the apparent anomaly in the ratio of contained muon neutrino to electron neutrino interactions as seen by the Kamiokande [1] and IMB detectors [2]. The Frejus [3] and NUSEX [4] detectors, however, have observed the expected number of contained events with smaller statistics. The Soudan II Collaboration

---

(\*) Paper presented at the VII Cosmic Physics National Conference, Rimini, October 26-28, 1994.

has reported preliminary results which are in agreement with the IMB and Kamiokande observations [5].

Finally, several models exist which predict a flux of VHE and UHE  $\nu$ 's from astrophysical sources (galactic, like neutron stars, black holes and young supernovae remnants; extragalactic, like Active Galactic Nuclei). Also if these neutrinos travel through very long distances, the probability of their being either deviated or stopped is very low, given the very small cross-section and the low interstellar medium density.

The MACRO underground detector is instrumented for the detection of neutrino burst from supernovae explosion, using the large amount of liquid scintillator (600 tons). However, in this paper we focus mainly on the detection of atmospheric  $\nu$ 's in different energy intervals, and the search for possible cosmic point sources of neutrinos.

## 2. – The MACRO Experiment as a $\nu$ detector

MACRO [6] (Monopole, Astrophysics and Cosmic Ray Observatory) is a large-area underground detector, with a mean rock overburden of  $\sim 3700 \text{ hg cm}^{-2}$ , located at the Laboratori Nazionali del Gran Sasso in Italy. It consists of 6 supermodules (SM) with overall dimensions of  $72 \text{ m} \times 12 \text{ m} \times 9 \text{ m}$ . Each SM has a lower part of 4.8 m height and an upper part (*Attico*) of 4.2 m. The lower detector consists of a large rectangular box with an outer shell of liquid scintillator counters and 6 layers of streamer tubes; it has 10 horizontal layers of plastic streamer tubes distributed inside the box. The eight inner streamer tube planes are separated by passive absorbers ( $60 \text{ g cm}^{-2}$  of iron and rock) in order to set a minimum threshold of about 1 GeV for vertical muons crossing the detector. The streamer tubes are used for tracking, and are equipped with readout electronics on both the wires (3 cm cells) and on cathode strips, placed at a stereo angle of  $27^\circ$  with respect to the wires. The intrinsic angular resolution (studied using down-going muons [6]) for reconstructed tracks in the detector with at least four planes of streamer tubes hit is  $0.14^\circ$  for wire tracks and  $0.29^\circ$  for strip tracks. The scintillator system for the lower part consists of 192 horizontal boxes of liquid scintillator ( $11.2 \text{ m} \times 0.73 \text{ m} \times 0.19 \text{ m}$ ) and 98 vertical boxes ( $11.1 \text{ m} \times 0.23 \text{ m} \times 0.43 \text{ m}$ ). After calibration, the time resolution for muons in a scintillator box is about 500 ps which corresponds to a position resolution along the length of the box (determined using the difference in time at the two box ends) of about 11 cm.

To run as a neutrino detector, MACRO needs both the streamer tubes and scintillator subsystem working with high efficiency. The data we present here refers to three different running periods without *Attico*. The first (*Period I*) used one SM and lasted from March 1989 until November 1991, with a live time of about 1.4 y. The second (*Period II*) was between March 1992 to December 1992, when the detector was under construction. The third (*Period III*) is from December 1992 until June 1993, using 6 SM with a live time of 0.42 y.

Neutrino interactions can be detected via the production of a charged lepton through the process  $\nu_\mu N \rightarrow \mu X$ . Referring to fig. 1, we can thus distinguish four different event topologies: 1) upward throughgoing muons; 2) upward going stopping muons; 3) partially contained upward going muons; 4) partially contained downward going muons.

For topologies 1) and 2) the  $\nu_\mu$  interaction happens in the rock below the apparatus, while in 3) and 4) it happens in the 5 kton of the passive absorber inside the apparatus. The neutrino average energy for topologies 2) and 3) is in a region of particular interest for the atmospheric neutrino problem. It must be noted that MACRO is not able to

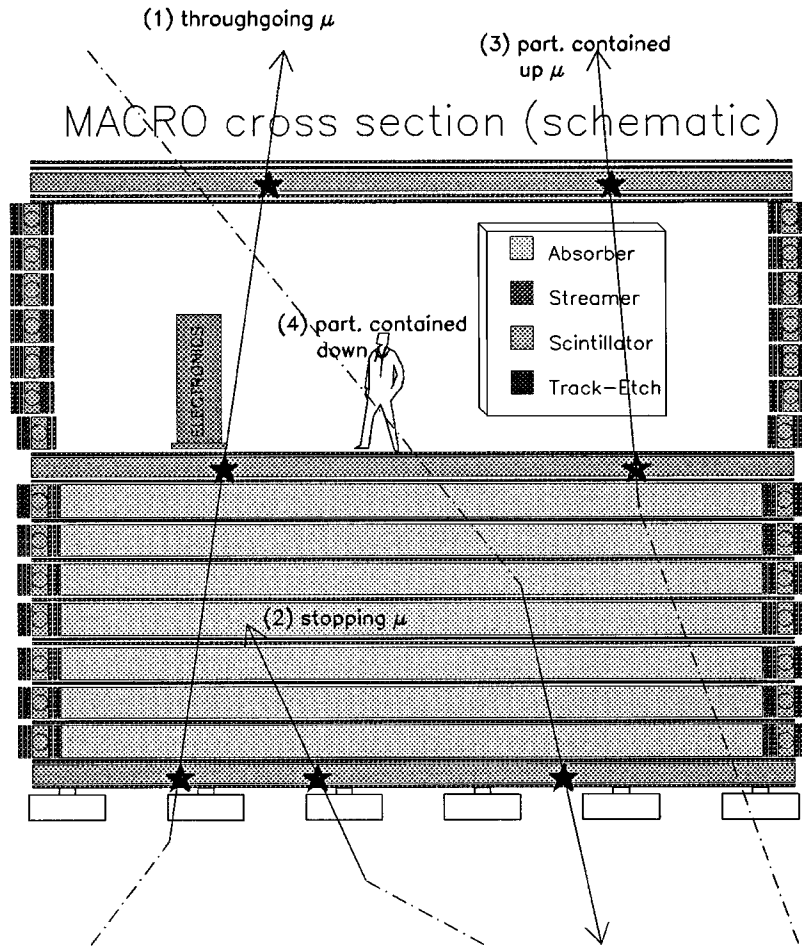


Fig. 1. – MACRO cross-section. The different neutrino-induced muon topologies are reported (see text). The stars indicate a scintillator hit.

distinguish between upward going stopping muons (2) and partially contained downward going muons (4). Partially contained upward going muons (3) can be collected only with the *Attico* part of the apparatus, which is taking data from Summer 1994. A small amount of  $\nu_e$  and  $\bar{\nu}_e$  interactions inside the detector can also produce a detectable signal. The possibility of distinguishing between muon neutrino and electron neutrino interactions is at present under study.

For each topology of neutrino-induced events, using a Monte Carlo (MC) simulation we evaluated the neutrino energy spectra which produce a detectable muon in MACRO. The MC consists of four parts: i) an atmospheric neutrino flux; the so-called Bartol (low and high energy) flux was used [7]; ii) the  $\sigma_{\text{tot}}^{\text{c.c.}}$  neutrino cross-section; iii) the propagation of the produced muon; this has been done using the energy loss calculation in standard rock of Lohmann *et al.* [8]; iv) a full simulation of the detector response, using a GEANT [9] based simulation program.

The charged current (c.c.) cross-section for the  $\nu$  interactions has been calculated

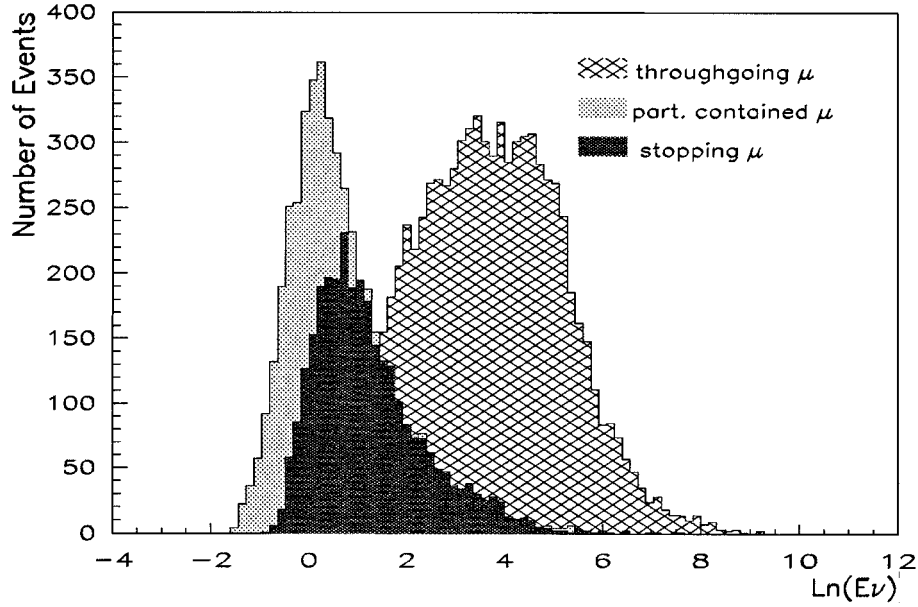


Fig. 2. – Neutrino energy spectra which produce a detected muon in MACRO. Energy in GeV.

as [10]

$$(1) \quad \sigma_{\text{tot}}^{\text{c.c.}} = \sigma_{\text{q.e.}} + \sigma_{1\pi} + \sigma_{\text{D.I.S.}}$$

$\sigma_{\text{q.e.}}$  = c.c. quasi-elastic scattering ( $\nu N \rightarrow lN'$ ), which take into account also the lepton mass, the Fermi momentum, the Pauli exclusion principle and nuclear binding;  $\sigma_{1\pi}$  = c.c. at the  $\Delta$ -resonance ( $\nu N \rightarrow lN'\pi$ ,  $W \leq 1.4$  GeV);  $\sigma_{\text{D.I.S.}}$  = c.c. deep inelastic scattering, calculated using the Morfin and Tung parton distribution set S1 [11].

In fig. 2 the distribution of the neutrino energies which produce a detected muon in MACRO for the different event topologies (partially contained events have been added) is presented. Due to the systematic uncertainty on the  $\nu$  flux, on cross-section and apparatus acceptance, the statistical sample in fig. 2 is for 40 to 50 years of data taking with the full apparatus. In column 2 and 3 of table I are reported the  $\nu$  energy intervals in which 90% of the signal is contained and the  $\nu$  mean energy for each event topology. The 5% of the

TABLE I. – Column 2: neutrino energy interval for 90% of the neutrino-induced muons detected in MACRO (see text). Column 3: mean neutrino energy in the interval. Column 4: accessible value in the  $\Delta m^2$  region for neutrino oscillations.

Event topology	90% of $\nu$ signal GeV	$\langle E_\nu \rangle$ GeV	$\Delta m^2 \sim \langle E_\nu \rangle / \langle L \rangle$ eV <sup>2</sup>
1	$4 < E_\nu < 500$	80	$10^{-2}$
2	$0.85 < E_\nu < 35$	5.0	$10^{-3}$
3	$0.65 < E_\nu < 22$	3.7	$10^{-3}$
4	$0.50 < E_\nu < 15$	2.3	$10^{-1}$

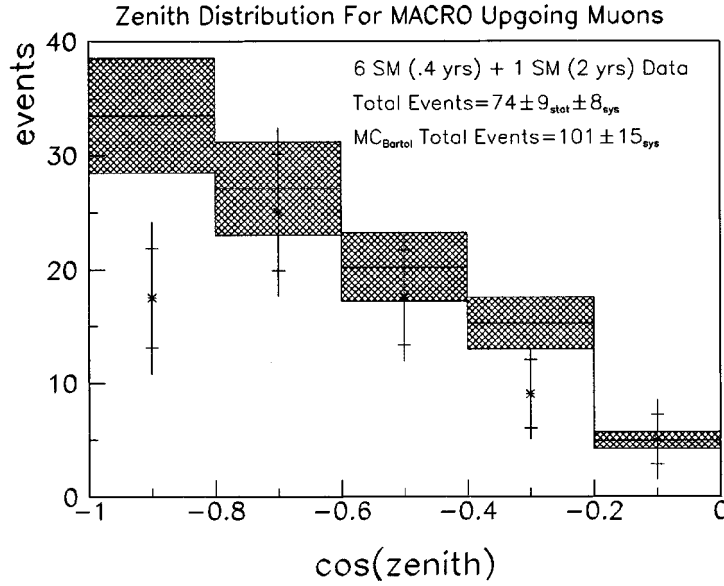


Fig. 3. – Distribution of  $\cos(\text{zenith})$  for the upgoing muon flux for the combined data of *Period I* and *III*. The extensions to the statistical error bars are the point-by-point estimates of the systematic error. The Monte Carlo expectation using the Bartol flux is shown in the shaded regions with a  $\pm 15\%$  systematic error range.

lowest and the 5% of the highest energy events were excluded.

Neutrinos which give rise to upward going muons (topology from 1 to 3) have a typical path length  $\langle L \rangle \sim 10^4$  km from the production point to the detector, while  $\langle L \rangle \sim 10$  km for partially contained downward going muons. The mean distance and the neutrino energy set the scale for the region in  $\Delta m^2$  accessible to each topology in the expression for the oscillation probability (column 4 of table I).

### 3. – Neutrino-induced muon measurements

**3.1. Upward going muons.** – This measurement was done using the time of flight between two layers of scintillation counters. Data from *Period I* and *Period III* were used. A rejection factor of at least  $10^5$  is necessary to separate the upgoing neutrino-induced muons from the ordinary downgoing atmospheric muons. The path length  $D$  between scintillator boxes is calculated using the streamer tube tracks. The velocity of each particle is then simply  $\beta c = D / (T_b - T_u)$ , where  $T_b$  ( $T_u$ ) is the mean time measured in the lower (upper) scintillator plane. Using this convention, up throughgoing  $\mu$  have a  $1/\beta = -1$ . Figure 3 shows the zenith angle distribution of upgoing muon events for the combined data set of *Period I* and *III*, compared to the Monte Carlo expectation. The total number of detected and expected events are also shown in fig. 3. The systematic error on the data reflects the uncertainty in the acceptance, efficiency factor and background subtraction for each point.

The integrated number of detected events in all zenith bins agrees with Monte Carlo predictions to within  $1.1\sigma$ . The  $\chi^2$ -test applied to the experimental zenith distribution compared to the Monte Carlo gives a  $\chi^2 = 8.0$ . For 5 D.o.F (no oscillation hypothesis) the

TABLE II. – Number of detected up stopping muons in the period III data sample vs. the crossed number of streamer planes and crossed detector thickness.

Number of planes	$\text{g cm}^{-2}$	Number of events
2	$\sim 40$	18
3	$\sim 100$	9
4	$\sim 160$	3
5	$\sim 220$	3
6	$\sim 280$	2

probability of this  $\chi^2$  is 16%.

3.2. *Stopping and partially contained muons.* – Upward going stopping and partially contained muons (hereafter *up stopping muons*) have the same topology in the apparatus, and can be detected if the muons cross a scintillator counter in the bottom plane and at least two streamer tube planes. The search for *up stopping muons* was done using only data of *Period III*, and it is still in progress. The analysis takes into account several detector's effects (gaps, inefficiencies, etc.) that could simulate a stopping muon. In table II the number of detected events vs. the number of crossed streamer tube planes is reported (*i.e.* different energy threshold for the muon).

A possible source of background for these events is the large-angle pion production due to downward going muon interaction in the rock below the detector. An example of a downward going muon plus a backward going  $\pi$  (identified studying the crossing time on the scintillator counters) is presented in fig. 4. During the considered data taking period 38 event of this kind were detected. A background event can happen when the downward particle does not intersect the detector. Using a phenomenological Monte Carlo, a rough estimate of this background was evaluated as  $4 \pm 2$  background events, and affects mainly the configuration of the first row of table II.

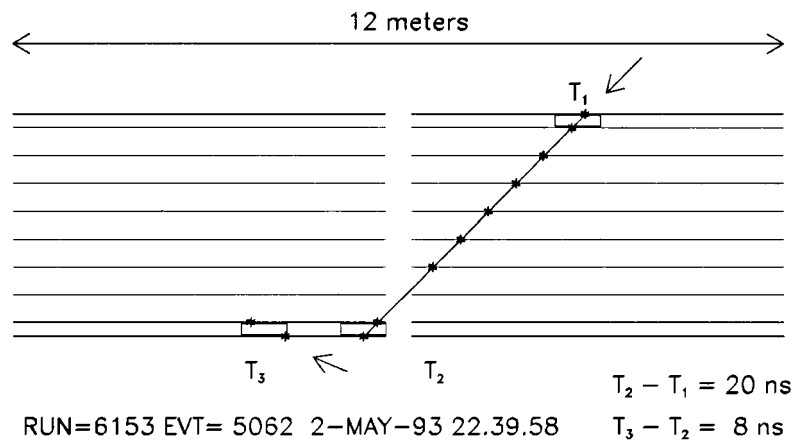


Fig. 4. – Downward going muon with a backward pion. The time measurement in the scintillator counters suggests a flight direction as indicated by the arrows.

#### 4. – Search for astrophysical point sources of $\nu$

A search has been made for upgoing muons produced by neutrinos coming from celestial objects using the whole data sample. The very good angular resolution of MACRO allows for tight angular bins around possible sources. The angular difference between the detected  $\mu$  direction and the parent  $\nu$  depends on the source spectral index, the multiple scattering of the muon in the crossed rock and the detector intrinsic angular resolution. We calculated via Monte Carlo that, given a spectral index between 2.0 and 2.2 [12], a search cone of  $3^\circ$  (half-width) around the direction of a source will include 90% of the muons observed in MACRO from that source. The expected background (due, in this case, to atmospheric neutrinos and calculated using the data itself) inside of each search cone is roughly 0.1 *event* for the considered data taking period.

We have investigated 13 different sources (CygX-3, HerX-1, Crab, Geminga, SS433, ScoXr-1, Galactic Center, VelaXR-1, Vela Pulsar, CenXR-1, LMCX-4, SN1987A, LMCX-2). No events were found within the  $3^\circ$  search bin centered on each of the sources listed. Flux upper limits (90% C.L.) from these sources range from  $6 \cdot 10^{-13} \text{ cm}^{-2}\text{s}^{-1}$  (CygX-3) to  $2.4 \cdot 10^{-14} \text{ cm}^{-2}\text{s}^{-1}$  (LMC).

In addition, we have made a search for clusters of events independent of whether they lie near some known object. No statistically significant cluster of events has been found.

#### REFERENCES

- [1] HIRATA K. S. *et al.*, *Phys. Lett. B*, **280** (1992) 146.
- [2] CASPER D. *et al.*, *Phys. Rev. Lett.*, **66** (1991) 2561.
- [3] BERGER CH. *et al.*, *Phys. Lett. B*, **245** (1990) 305; **227** (1989) 489.
- [4] AGLIETTA M. *et al.*, *Europhys. Lett.*, **8** (1989) 611.
- [5] ALLISON W. *et al.*, ANL-HEP-CP-93-34.
- [6] AHLÉN S. P. *et al.*, *Nucl. Instrum. Methods A*, **324** (1993) 337.
- [7] FRATI W. *et al.*, *Phys. Rev. D*, **48** (1993) 1140; GAISSER T. K., private communication.
- [8] LOHMANN W. *et al.*, CERN-EP/85-03, Mar, 1985.
- [9] BRUN R. *et al.*, CERN report DD/EE84-1, 1987.
- [10] LIPARI P., LUSIGNOLI M. and SARTOGO F., *Phys. Rev. Lett.*, **74** (1995) 4384.
- [11] MORFIN J. G. and TUNG W. K., *Z. Phys. C*, **52** (1991) 13.
- [12] STANEV T., *Nucl. Phys. B*, **35** (1994) 185.